Diffusion Barriers Limit the Effect of Mobile Calcium Buffers on Exocytosis of Large Dense Cored Vesicles

Karel S. Kits,* Theo A. de Vlieger,* Bob W. Kooi,# and Huibert D. Mansvelder*
*Membrane Physiology Section, Research Institute Neurosciences, and #Department of Theoretical Biology, Faculty of Biology, Vrije Universiteit Amsterdam, De Boelelaan 1087, 1081 HV Amsterdam, The Netherlands

ABSTRACT Fast exocytosis in melanotropic cells, activated by calcium entry through voltage-gated calcium channels, is very sensitive to mobile calcium buffers (complete block at 800 μM ethylene glycol bis(β-aminoethyl ether)-*N,N,N′N′*-tetraacetic acid (EGTA)). This indicates that calcium diffuses a substantial distance from the channel to the vesicle. Surprisingly, 1,2-bis(2-aminophenoxy)ethane-*N,N,N′,N′*-tetraacetic acid (BAPTA), having a similar K_D for calcium as EGTA but a ~100 times faster binding rate, blocked exocytosis only twice as effectively as EGTA. Using computer simulations, we demonstrate that this result cannot be explained by free diffusion and buffer binding rates. We hypothesized that local saturation of calcium buffers is involved. A diffusion barrier for both calcium and buffer molecules, located 50–300 nm from the membrane and reducing diffusion 1000 to 10,000 times, generated similar calcium concentrations for specific concentrations of EGTA and BAPTA. With such barriers, calcium rise phase kinetics upon short step depolarizations (2–20 ms) were faster for EGTA than for BAPTA, implying that short depolarizations should allow exocytosis with 50 μM EGTA but not with 25 μM BAPTA. This prediction was confirmed experimentally with capacitance measurements. Coupling exocytosis to calcium dynamics in the model, we found that a barrier with a ~3000 times reduced diffusion at ~130 nm beneath the membrane best explains the experimentally observed effects of EGTA and BAPTA on block and kinetics of release.

INTRODUCTION

The final step in regulated secretion involves excitation-secretion coupling, which comprises, through activation of voltage-gated calcium channels, the triggering of calcium-dependent fusion of docked vesicles with the plasma membrane. In addition, calcium facilitates predocking and docking of vesicles (reviews by Schweizer et al., 1995; Zucker, 1996; Stanley, 1997; Neher 1998). In fast synapses, operating through classical transmitters like γ-aminobutyric acid and glutamate, it appears that calcium channels are closely linked to docked vesicles, due to interactions between N- and Q-type high voltage-activated Ca^{2+} channels and syntaxin, one of the peptides of the fusion machinery (Leveque et al., 1994; Sheng et al., 1994; Bezprozvanny et al., 1995). As a result, rises in calcium levels induced by channel activity occur in the immediate vicinity of the low-affinity, calcium-dependent peptides that are responsible for fusion. Thus, a very rapid fusion and release process is triggered, restricted to the so-called microdomain of calcium, arising upon channel opening.

In contrast, although regulated release of large dense core vesicles (usually containing peptide messengers) is subject to a similar excitation-release coupling mechanism, it proceeds at a much slower pace (Chow et al., 1992; Heinemann et al., 1994; Thomas et al., 1993a; Neher and Zucker, 1993). It is assumed that the distance between calcium channels and the fusion peptide machinery is much larger, which implies that calcium ions must diffuse over some distance before they can act upon the fusion peptides (Chow et al., 1994, 1996; Seward and Nowycky, 1995, 1996; Seward et al., 1995). Thus, mobile calcium buffers like ethylene glycol bis(β-aminoethyl ether)-*N,N,N′,N′*-tetraacetic acid (EGTA) and 1,2-bis(2-aminophenoxy)ethane-*N,N,N′,N′*-tetraacetic acid (BAPTA) will affect the fusion of large dense core vesicles with the plasma membrane (Klingauf and Neher, 1997; Neher 1998). In line with this assumption, we observed that both concentration and affinity of the mobile calcium buffer determine how secretion in neuroendocrine cells is affected by the buffer (Mansvelder and Kits, 1998). In rat pituitary melanotropes, EGTA buffering interferes with secretion at low concentrations, causing a progressive decrease in release at 100–800 μM. However, BAPTA, despite acting about 100 times faster than EGTA, was only twice as effective in blocking exocytosis.

In the present study we asked what mechanism is responsible for the discrepancy between the large difference in Ca-binding rates of the buffers on the one hand and their similar effects on exocytosis on the other hand. Because our results pertain to rapid exocytosis occurring within 40 ms of the onset of stimulation, it is ruled out that a steady state condition applies, where it is not the difference in binding rate but rather the much smaller difference in affinity that is relevant (Nowycky and Pinter, 1993). Using computer simulations of calcium kinetics and exocytosis, we first tested whether the combined effects of calcium and buffer diffusion could explain this discrepancy. This would imply that different concentrations of EGTA and BAPTA would yield similar calcium levels at the site of release. Second, we tested whether saturation of the mobile calcium buffer

Received for publication 30 July 1998 and in final form 7 December 1998.
Address reprint requests to Karel S. Kits, Membrane Physiology Section, Research Institute Neurosciences, Vrije Universiteit Amsterdam, De Boelelaan 1087, 1081 HV Amsterdam, The Netherlands. Tel.: 31-20-44-47096; Fax: 31-20-44-47123; E-mail: ksk@bio.vu.nl.

0006-3495/99/03/1693/13 $2.00

would play a role. Finally, we tested whether the different kinetics of exocytosis predicted by the model with either EGTA or BAPTA are in agreement with experimental measurements using capacitance recording.

We simulated spatial and temporal changes in intracellular calcium levels (referred to as calcium profiles and calcium kinetics) in melanotropic cells. To this end we made use of a shell model applied to a spherical cell 13 μm in diameter. Klingauf and Neher (1997) have shown that such a shell model can be used to estimate the lateral diffusion for distances $\geq$100 nm from the channel. To induce saturation of calcium buffers in the model, we introduced diffusion barriers for calcium ions and buffer molecules. To simulate exocytosis we used a model that describes the final stage of exocytosis as a four-step process characterized by a third-order calcium dependence and an irreversible, calcium-independent final fusion step (cf. Thomas et al., 1993b; Heinemann et al., 1994; Klingauf and Neher, 1997).

Our results demonstrate that a limited difference between the effects of EGTA and BAPTA on exocytosis is obtained only if local saturation of mobile calcium buffers is allowed. Saturation will occur when diffusion barriers, for instance, formed by vesicles and calcium stores, are present close to the membrane.

MATERIALS AND METHODS

Experimental studies

Experimental methods employed to obtain primary cultures of rat pituitary melanotropes have been elaborately described previously (Keja et al., 1991; Mansvelder et al., 1996). In brief, intermediate lobe cells from adult male Wistar rats (200–300 g, Harlan CPB, Zeist, The Netherlands) were dissociated enzymatically, followed by trituration. Cells were cultured on poly-L-lysine coverslips (7 $\times$ 7 mm) in a medium consisting of Biorich I (Flow), $NaHCO_3$ 26.2 mM, Ultroser G 5% (Life Technologies, Gaithersburg, MD), penicillin G 200 U/ml (Sigma, St. Louis, MO), streptomycin 50 μg/ml (Sigma), and cytosine arabinose 1 μM (Sigma), adjusted to pH 7.2 with NaOH. Cells were maintained at 37°C under 5% CO_2 in humidified air.

Calcium current recordings and capacitance measurements were made using an Axopatch 200A amplifier (Axon Instruments, Foster City, CA) and a Digidata 1200 interface (Axon Instruments). Capacitance measurements were made to conform to Joshi and Fernandez (1988), Fidler and Fernandez (1989), and Fidler Lim et al. (1990). Analysis of capacitance measurements was performed as described elaborately by Mansvelder and Kits (1998). All experiments were performed at 32–34°C. Experimental solutions to obtain isolated calcium currents are given in Mansvelder and Kits (1998).

Simulations

Simulation studies were performed using NEURON, a software package specially designed for detailed biophysical neuron simulations (Hines, 1989). Mobile calcium buffering, diffusion of calcium and calcium chelators, and the process of exocytosis were incorporated as compiled mechanisms from *nmodl* files included in the standard version of NEURON, which is in the public domain. The NEURON package uses cylindrical cells. We altered its cylindrical coordinate system to a spherical one, although the differences in results obtained with the cylindrical and spherical models were small. Cells were conceived as being built up from concentric shells (n = 500). Values of relevant parameters within a shell are constant, with transitions occurring between shells. Calcium influx was assumed to occur homogeneously over the cell membrane. We simulated diffusion barriers by altering the diffusion coefficient between two consecutive shells. The secretion model of Klingauf and Neher (1997) was adapted to fit the results of Thomas et al. (1993b). If a diffusion barrier was used, we always took the calcium concentration of the shell just peripheral to the barrier as input for the secretion model. Table 1 lists the numerical values of all parameters used in these simulations. As far as possible, values used were taken from experimental data on melanotropes. Following are the essential equations used in the model.

Buffering was modeled by

$$\{d[Ca]_i/dt\} = k_{off}[CaB]_i - k_{on}[Ca]_i[B]_i) \quad (1)$$

where $[Ca]_i$ is the calcium concentration in shell i, $[B]_i$ is the buffer concentration in shell i, $[CaB]_i$ is the concentration calcium bound to buffer in shell i, and k_{off} and k_{on} are on and off rates of the binding of buffer and calcium. In all simulations, initial concentrations of a particular buffer were equal in every shell.

TABLE 1 Parameters used for simulations

Name	Definition	Standard value
Cell properties		
R	Cell radius[1,2]	6.5 μm
$N_{channel}$	Number of calcium channels per cell[2]	1250
$G_{channel}$	Conductance of calcium channel[2]	24 ps
i_{Ca}	whole cell calcium current[3]	fitted from experimental current
$[Ca^{2+}]_i$	basal calcium concentration[4]	0.1 μM
Diffusion		
D_{Ca}	calcium diffusion coefficient[4]	0.4 μm^2/ms
D_B	buffer diffusion coefficient[4]	0.2 μm^2/ms
Buffering		
k_{on} (EG)	rate constant of Ca^{2+} binding by EGTA[5]	1 $mM^{-1}ms^{-1}$
k_{on} (BA)	rate constant of Ca^{2+} binding by BAPTA[6]	100 $mM^{-1}ms^{-1}$
K_D (EG), K_D (BA)	dissociation constant EGTA and BAPTA[5,6]	0.2 μM
k_{on} (fixed buffer)	rate constant of Ca^{2+} binding by fixed buffer[4]	10^8 $M^{-1}s^{-1}$
K_D (fixed buffer)	dissociation constant[4]	10 μM
[EG]	total EGTA buffer concentration	50–800 μM
[BA]	total BAPTA buffer concentration	25–400 μM
Secretion		
B_0	pool of release ready vesicles[7]	250 fF
k_b	rate constant of calcium binding[4]	8 $mM^{-1}ms^{-1}$
k_u	rate constant of calcium dissociation[4]	0.08 ms^{-1}
k_{fus}	rate constant for vesicle fusion[8]	0.025 ms^{-1}
Temperature		
Q_{10}	temperature dependence for all rate constants[5]	3

[1]Keja et al., 1991
[2]Keja and Kits, 1994
[3]Mansvelder and Kits, 1998
[4]cf. Nowycky and Pinter, 1993
[5]cf. Smith et al., 1984
[6]cf. Tsien et al., 1980
[7]cf. Thomas et al., 1993a,b
[8]cf. Klingauf and Neher, 1997

Diffusion of calcium and calcium buffers was modeled as

$$\{d[S]_i/dt\} = (D_s/V_i\delta)\{A_{i-1}([S]_{i-1} - [S]_i) - A_i([S]_i - [S]_{i+1})\} \quad (2)$$

where $[S]_i$ is the concentration of the diffusing molecule, D_s is the diffusion rate of the diffusing molecule, V_i is the volume of shell *i*, δ is the distance between the centers of two consecutive shells, and A_i is the surface area of shell *i* over which diffusion is taking place.

Because the experiments were carried out at a temperature of 33°C, all rate constants, including those of the buffers (Smith et al., 1984), were adapted using a Q_{10} of 3. Secretion was expressed in fF per million calcium ions.

RESULTS

Calcium dynamics with EGTA and BAPTA

Previously we showed that high micromolar concentrations of both EGTA and BAPTA completely block exocytosis (Mansvelder and Kits, 1998). It was concluded that the site of calcium entry is relatively far away from the site of the calcium sensor, triggering vesicle fusion. Calcium diffusion in that case takes long enough to allow the buffers to interact with calcium. This result implies that only changes in calcium levels at distances >100 nm from the channel are relevant for secretion. Klingauf and Neher (1997) showed that for such distances, calcium diffusion can be simulated in a concentric shell model such as that described previously by Sala and Hernandez-Cruz (1990) and Nowycky and Pinter (1993). The model assumes homogenous calcium distribution within a shell and transitions at shell boundaries. Consequently, only radial diffusion is taken into account. Calcium influx was derived from the calcium current recorded under whole cell voltage clamp (see Fig. 2 *C*, inset). Depolarizing pulses to a test potential of +10 mV lasted 40 ms, in accordance with the protocol used in previous experiments (Mansvelder and Kits, 1998).

Our experimental results indicate that the mobile calcium buffers EGTA and BAPTA differ by no more than a factor of 2 in blocking exocytosis (Fig. 1). The limited difference between the effects of EGTA and BAPTA on release is intriguing, because EGTA and BAPTA have k_{on} rates that differ by a factor of 100. Obviously, this result cannot be explained by the different calcium binding rates of both chelators. However, the similar affinities of both buffers for calcium also fail to explain our data because only rapid release, occurring during the dynamic phase of calcium kinetics, was measured (Nowycky and Pinter, 1993). As a starting point, we therefore asked whether this experimental result is explained by diffusion and buffer rate constants. This would require that a 40-ms depolarization lead to similar calcium levels near the site of release when either EGTA or BAPTA (which differ by a factor of 2 in concentration) is used. Such a condition would clearly lead to equal amounts of release and capacitance change. Fig. 2, *A* and *B*, shows the time course of changes in submembranous calcium levels in response to a 40-ms depolarization to +10 mV with either 400 μM EGTA or 200 μM BAPTA. These

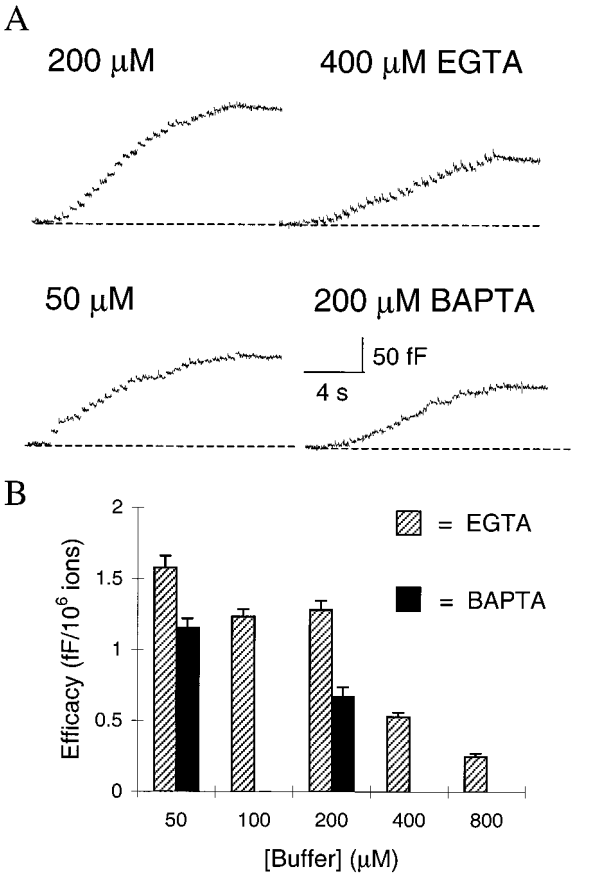

FIGURE 1 BAPTA is only twice as efficient as EGTA in blocking calcium-dependent exocytosis in dissociated melanotropes. (*A*) Capacitance traces in response to series of 25 depolarizing steps of 40 ms duration with various concentrations of EGTA or BAPTA in the pipette solution, as indicated. (Holding potential −80 mV, depolarizing steps to +10 mV, 0.5-s intervals between pulses within a series.) (*B*) Average efficacy (± SEM) of the coupling of calcium influx to exocytosis expressed as the increase in capacitance per million calcium ions at various concentrations of EGTA or BAPTA. Data were obtained by calculating the mean response to the 25 pulses of a series and averaging these mean values for 5 to 13 cells.

simulations demonstrate that over the entire pulse duration, strongly different calcium levels are obtained for both conditions. Fig. 2 *C* shows the calcium profile beneath the cell membrane at the end of a 40-ms pulse. Calcium levels are different up to ~2500 nm from the site of entry, implying that nowhere near the cell membrane does a condition of equal $[Ca]_i$ occur. These results imply that diffusion of calcium and calcium buffers is insufficient to explain why these two chelators differ by only a factor of 2 in affecting release.

Because endogenous fixed calcium buffers will play a role in determining the distribution of calcium ions in melanotropes, we repeated these simulations with a relatively fast, immobile buffer added to the model to supplement the mobile buffers (cf. Nowycky and Pinter, 1993). The results are given in Fig. 3. With 750 μM immobile buffer added to the cell, calcium kinetics are still different for the EGTA

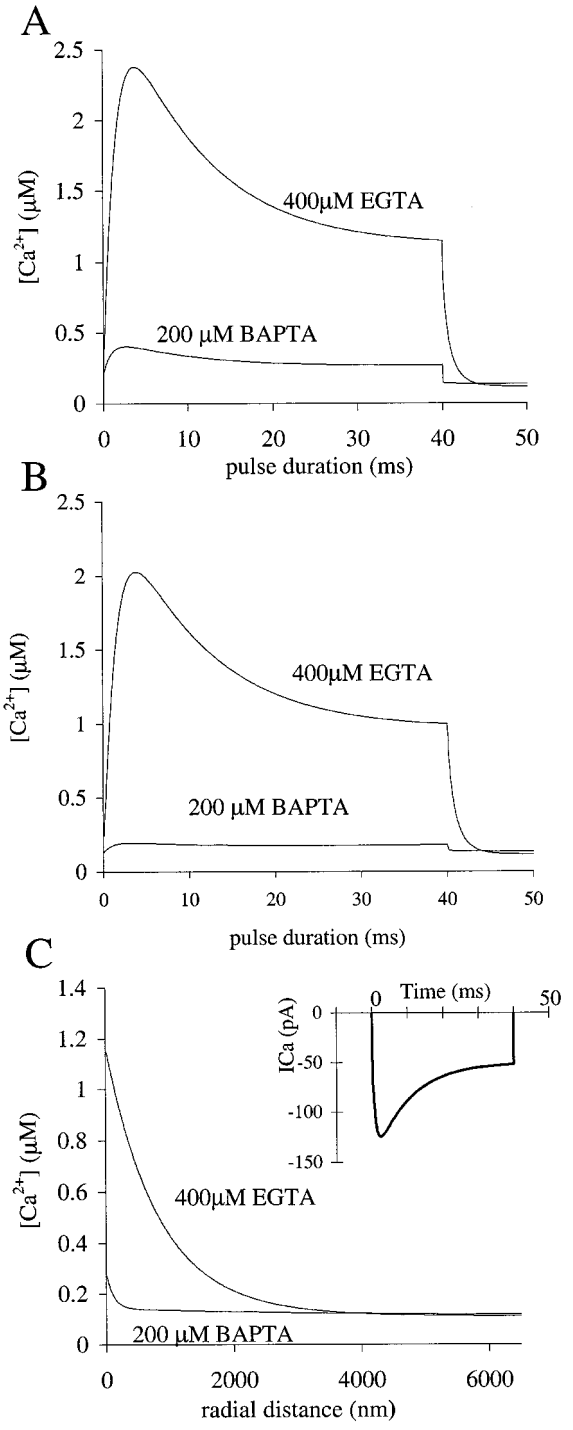

FIGURE 2 Diffusion and buffer properties do not explain equal exocytosis with 400 μM EGTA or 200 μM BAPTA. (*A*) Simulation of calcium kinetics in the first submembrane shell in the presence of 400 μM EGTA or 200 μM BAPTA. Chosen buffer concentrations result in equal amounts of exocytosis, measured experimentally as the capacitance increase at the end of a 40-ms depolarization. However, during the entire step pulse of 40 ms, there is no point at which calcium levels are equal under both conditions. (*B*) Like *A*, but now in the 10th submembranous shell. (*C*) Calcium profile beneath the cell membrane at the end of a 40-ms depolarization. Plotted is $[Ca^{2+}]_i$ at increasing radial distances from the cell membrane with either 400 μM EGTA or 200 μM BAPTA as mobile calcium buffer. Equal calcium concentrations occur only at considerable distance from the membrane (~2500 nm) and are not encountered at relevant distances. Inset: Idealization of the experimentally recorded calcium current in response to a 40-ms depolarization from a holding potential of −80 mV to a test potential of +10 mV. The current trace was constructed using *mh* kinetics. This idealized calcium current trace was used throughout in all simulations.

and BAPTA conditions during the entire pulse (Fig. 3, *A* and *B*). The calcium profile still displays considerable differences over a distance of ~1500 nm from the site of entry (Fig. 3 *C*). When even larger concentrations of fixed buffer were simulated, the point of convergence of the effects of 200 μM BAPTA and 400 μM EGTA on $[Ca^{2+}]_i$ shifted further toward the membrane, as illustrated in Fig. 3 *D*. However, the actual level of $[Ca^{2+}]_i$ at the point of convergence was invariably very close to the basal level ($\sim 10^{-7}$ M), which is obviously too low to induce exocytosis (Fig. 3 *D*). We conclude that when the effects of a fixed buffer are also taken into account, the experimental results are not explained by diffusion and buffer properties.

Buffer saturation

As a next step, we hypothesized that local saturation of buffers might play a role. Because the sites of calcium entry and release are dissociated by 100 nm or more, buffer saturation at the release sites will not occur under circumstances of normal, unhampered diffusion. In this respect, release in neuroendocrine cells differs strongly from synaptic release, where the total secretion complex is located within the 30-nm realm of the calcium domains. In order to cause saturation of calcium buffers, we introduced a diffusion barrier underneath the membrane, i.e., at the transition between two peripheral shells. A diffusion barrier would limit the spread of calcium and thus lead to prolonging of increased calcium levels underneath the membrane, the more so because, at the same time, it would hamper replacement of calcium-bound buffer molecules by free buffer. A diffusion barrier was modeled by reducing the diffusion constant for the transition to the $(N + 1)$th shell, i.e., at $N \times$ 13 nm from the cell membrane, and the strength of a barrier is expressed as the ratio of the diffusion constants for the transitions to shells $(N + 1)$ and N. Unless otherwise stated, $N = 10$.

The effect of barriers of various strengths was simulated. The results are shown in Fig. 4, *A* and *B*. Saturation of EGTA at 50 μM requires a barrier of 1/10,000. Under control conditions, BAPTA (at 25 μM) is saturated at the end of the 40-ms pulse, much like the situation described above for EGTA with a 1/10,000 barrier. However, while a barrier of 1/100 has little effect, a 1/1000 barrier strongly speeds up saturation, inducing complete saturation of BAPTA within 5 ms. The effect of barrier position is shown in Fig. 4, *C* and *D*. Even a barrier at shell 51 speeds up saturation, and the effect becomes stronger when the barrier is moved toward the cell membrane.

The next question then concerns the effects of a diffusion barrier on calcium kinetics. This is illustrated in Fig. 5, *A*

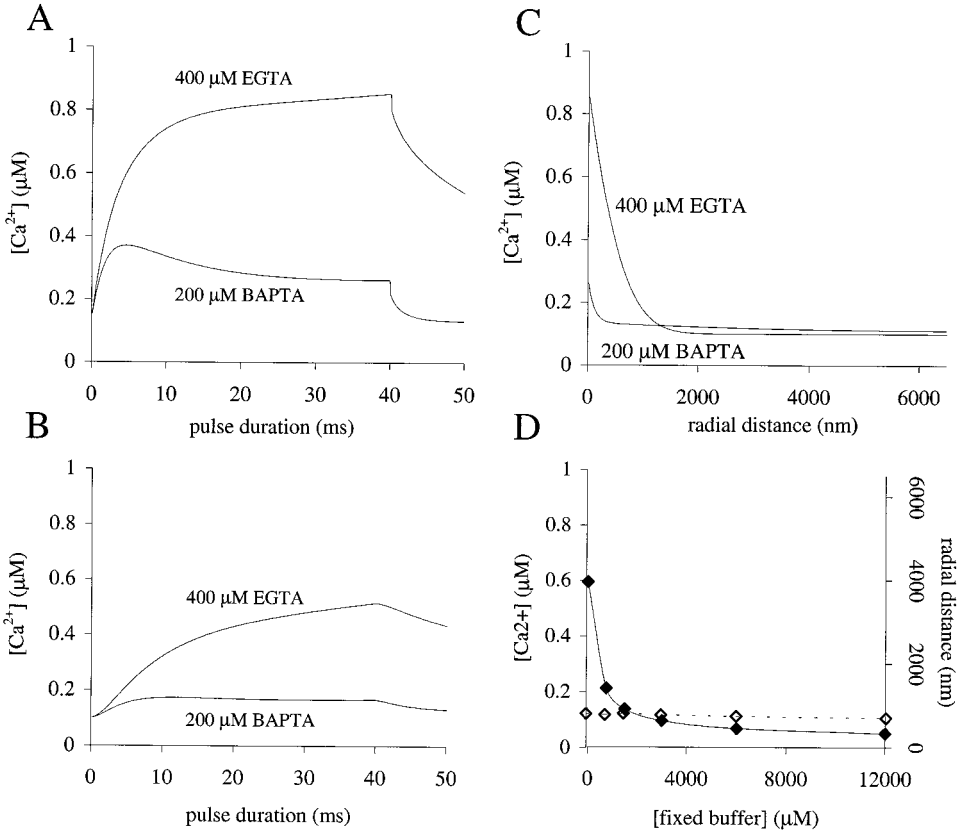

FIGURE 3 Addition of a fast fixed buffer does not induce calcium profiles that will lead to equal exocytosis with 400 μM EGTA or 200 μM BAPTA. (*A*) Simulation of calcium kinetics in the presence of 400 μM EGTA or 200 μM BAPTA and 750 μM fixed buffer (forward binding rate = $10^8 M^{-1}s^{-1}$; K_D = 10 μM). Illustrated are the time dependent changes in $[Ca^{2+}]_i$ in the first submembrane shell. With the fixed buffer, calcium levels remain strongly different under both conditions. (*B*) Like *A*, but now in the 10th submembranous shell. (*C*) Calcium profile beneath the cell membrane at the end of a 40-ms depolarization. With 750 μM of fixed buffer, equal calcium concentrations are obtained at ~1500 nm from the membrane, but not at relevant distances from the site of calcium entry. (*D*) Effect of fixed buffer concentration on convergence of the effects of 400 μM EGTA or 200 μM BAPTA. Plotted are the relation between $[Ca^{2+}]_i$ at the point of convergence (◇) and fixed buffer concentration as well as the relation between the location of the point of convergence (◆) (measured as radial distance from the cell membrane) and fixed buffer concentration. With increasing levels of fixed buffer the point of convergence shifts toward the membrane, but at the point of convergence $[Ca^{2+}]_i$ is invariably too low to induce exocytosis.

and *B*, for barriers of varying heights. It appears that a barrier of 1/1000 in shell 11 strongly affects the amplitude and the time course of changes in $[Ca]_i$, especially when BAPTA (25 μM) is used as a chelator. Under these conditions the time-dependent changes in $[Ca]_i$ are very similar for both buffers. A maximal $[Ca]_i$ level is reached after ~6 ms. Subsequently, $[Ca]_i$ decreases to about 75% of the maximum (traces 3 in Fig. 5, *A* and *B*). Increasing the barrier to 1/10,000 further increased the rise in $[Ca]_i$ for both buffers; there is even a point where the curves for BAPTA and EGTA cross each other. It thus appears that local diffusion buffers can strongly affect the amplitude and the time dependence of changes in $[Ca]_i$ and may create a situation where equal calcium levels are obtained for both chelators applied in a 1:2 ratio, thus explaining equal release. Fig. 5, *C* and *D* , shows that to induce similar calcium levels, the barrier should be located within ~300 nm of the membrane. With the barrier (height 1/10,000) at shell 51, similar calcium levels with EGTA and BAPTA are reached only at the end of the 40-ms pulse. With the barrier at shell 21 or 11, similar calcium levels are obtained after ~10 ms.

A second feature that becomes apparent from these simulations is that the kinetics of calcium differs for both chelators, especially with a high diffusion barrier. Thus, calcium levels rise immediately with EGTA as chelator, but there is a delay when BAPTA is used, due to the fast action of BAPTA that allows for complete buffering of all calcium during the first milliseconds of a pulse. The delayed and complex (at least biphasic) rising phase of $[Ca]_i$ with BAPTA as buffer is most clearly illustrated in Fig. 5 *D*.

Calcium kinetics and release

We then asked whether such differences in kinetics are reflected in the kinetics of release. To answer this question experiments were performed in which changes in capacitance were measured in response to depolarizing steps to +10 mV, increasing in duration from 2 to 40 ms (Fig. 6). These experiments were performed with either 50 μM EGTA or 25 μM BAPTA as mobile calcium buffer. Typical examples of the resulting current traces and capacitance are

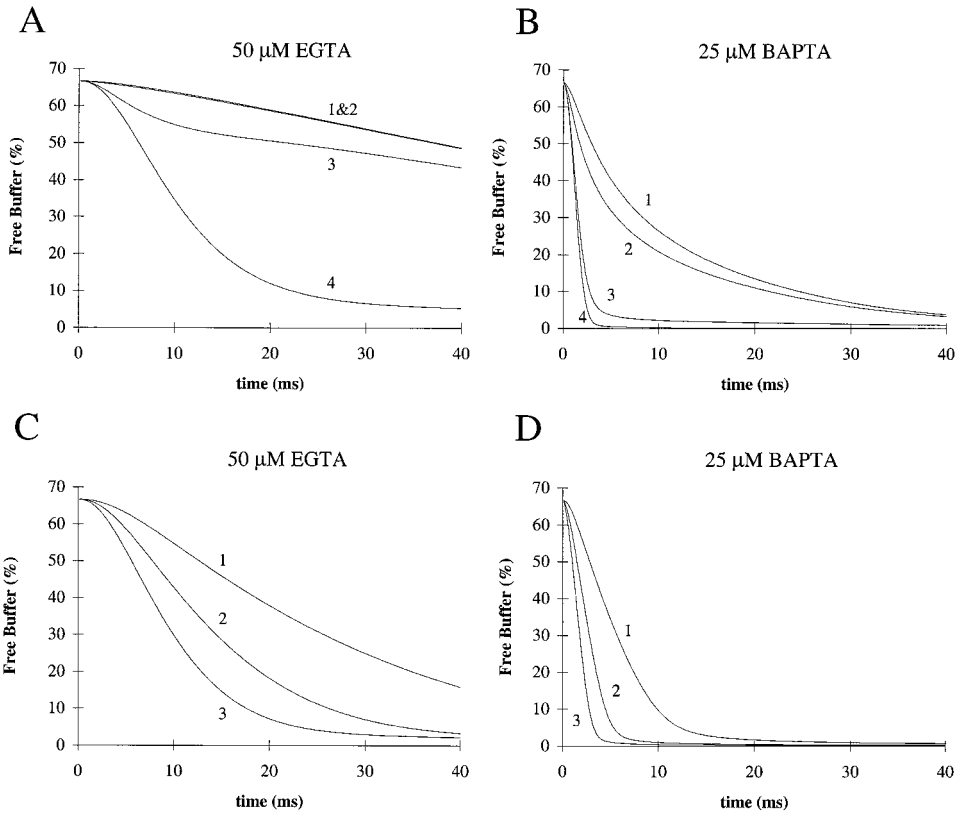

FIGURE 4 Introduction of a sufficiently large diffusion barrier enhances the rate and the amount of saturation of mobile calcium buffers during a 40-ms depolarization to +10 mV. (*A*) Percentage of free buffer as a function of time, applying various barrier heights (1, no barrier; 2, barrier height 1/100; 3, barrier height 1/1000; 4, barrier height 1/10,000) and using 50 μM EGTA as mobile calcium buffer. The barrier is located between shells 10 and 11. Plotted is the percentage of free buffer in shell 10. (*B*) Like *A*, but with 25 μM BAPTA. Increasing diffusion barrier strength progressively speeds up saturation until at 1/10,000, BAPTA is saturated within 3 ms and EGTA is nearly saturated within 20 ms. (*C*) Percentage of free buffer as a function of time, applying a barrier height of 1/10,000 at various positions (1, between shells 50 and 51; 2, between shells 20 and 21; 3, between shells 10 and 11) and using 50 μM EGTA as mobile calcium buffer. Plotted is the percentage of free buffer in shells 50, 20, and 10, respectively. (*D*) Like *C*, but with 25 μM BAPTA.

shown in Fig. 6 *A*, using 50 μM EGTA as calcium chelator, and Fig. 6 *B*, using 25 μM BAPTA as calcium buffer.

Fig. 7 summarizes the data for both conditions. Both capacitance changes (Fig. 7, *A1* and *B1*) and calcium currents (Fig. 7, *A2* and *B2*) are plotted against pulse duration. For both conditions, pulses of increasing duration progressively increase the capacitance. However, the shortest pulse, 2 ms, fails to increase capacitance with BAPTA as chelator and, in general, shorter pulse durations cause smaller capacitance changes with BAPTA than with EGTA (compare also Fig. 6, *A* and *B*). These differences become very clear when the efficacy of calcium ions to stimulate release (calculated as capacitance change divided by integral calcium current) is plotted as a function of pulse duration. Fig. 7, *A3* and *B3*, shows that a constant efficacy of 1 fF/million ions, independent of pulse duration, is obtained with 50 μM EGTA, whereas with 25 μM BAPTA the efficacy rises from zero at 2 ms pulses to slightly over 1 fF/million ions for pulses of 20 ms and longer. Thus, the experimental data reflect the differences in calcium kinetics that become apparent when the model includes a diffusion barrier.

Effects of a diffusion barrier on release

Our next aim was to define the strength and position of the barrier more closely. Therefore we simulated the above experiments by adding the release step to the model. Release was modeled as a four-step process in which fusion requires the cooperative binding of three calcium ions and a final calcium-independent step (cf. Thomas et al., 1993; Heinemann et al., 1994; Klingauf and Neher, 1997):

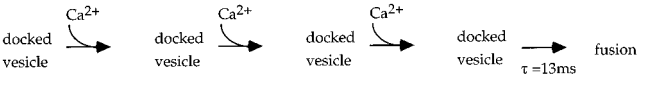

(3)

First we reassessed the height of the barrier. Fig. 8 plots the efficacy of release as a function of pulse duration for barriers increasing from 1/10 to 1/10,000 for both chelators. Obviously a barrier ~1/1000 offers the best approach of the experimental results, with largely pulse duration-independent efficacy for EGTA and increasing efficacy over the first 10 ms for BAPTA. Lower barriers yielded a strong dependence on pulse duration for both buffers, whereas higher barriers resulted in a constant efficacy, regardless of pulse duration, for both BAPTA and EGTA. The next step was to position the barrier at various distances beneath the membrane (Fig. 9). Here a distance of ~100 nm offered the best simulation of our experimental results. Barriers at larger distances failed to induce the experimentally observed independence of pulse duration for EGTA, apparently causing insufficient saturation in the submembranous area. As a final test we simulated the original experiments, in which the efficacy of calcium ions to induce release was measured as a function of buffer concentration. Again, barrier height and position were varied. Close approxima-

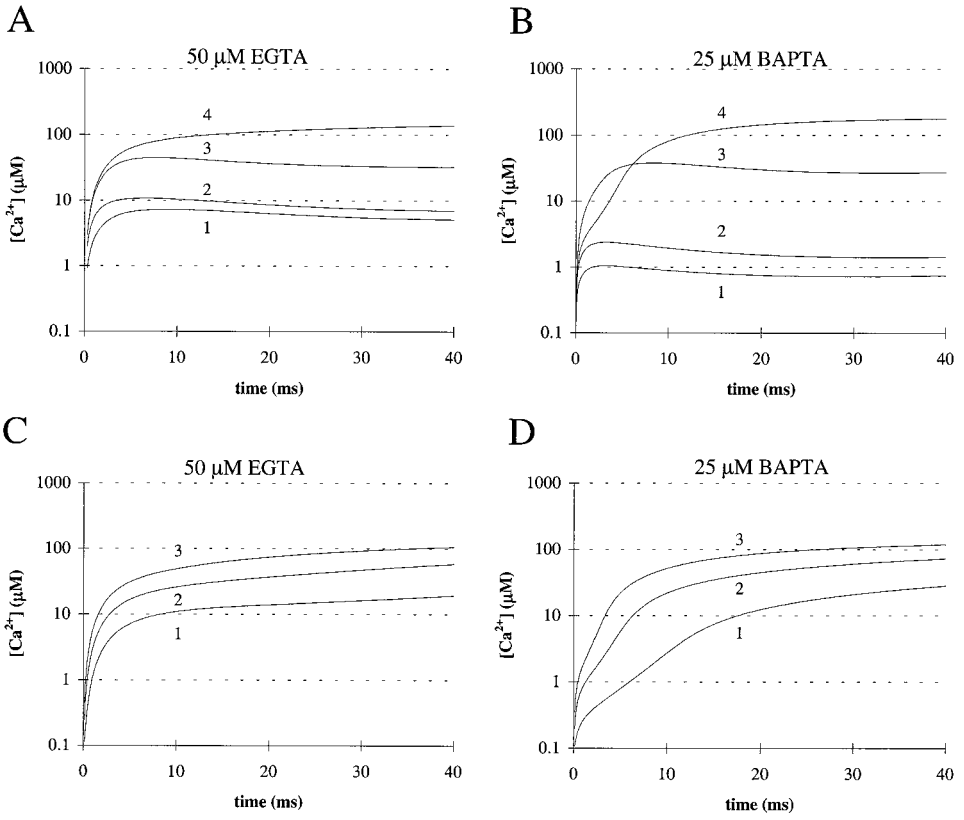

FIGURE 5 Effects of height and position of a diffusion barrier on calcium kinetics during a 40-ms depolarization. (*A*) Submembranous calcium levels during a 40-ms depolarization to +10 mV, applying various barrier heights (1, no barrier; 2, barrier height 1/100; 3, barrier height 1/1000; 4, barrier height 1/10,000) and using 50 μM EGTA as mobile calcium buffer. The barrier is located in shell 11. Plotted are the calcium levels in shell 10. (*B*) Like *A*, but with 25 μM BAPTA. Comparison of *A* and *B* shows that without a barrier and with a barrier of 1/100, calcium concentrations under both buffer conditions differ during the entire pulse length, with $[Ca^{2+}]_i$ being consistently much lower with 25 μM BAPTA than with 50 μM EGTA. With a barrier of 1/1000, $[Ca^{2+}]_i$ is strongly increased and only slightly higher for EGTA than for BAPTA. With a 1/10,000 barrier, the $[Ca^{2+}]_i$ lines for EGTA and BAPTA yield identical $[Ca^{2+}]_i$ after ~10 ms. C. Submembranous calcium levels during a depolarizing step to +10 mV, applying a barrier height of 1/10,000 at various positions (1, barrier location in shell 51; 2, in shell 21; 3, in shell 11) and using 50 μM EGTA as mobile calcium buffer. Plotted are calcium levels in shells 50, 20, and 10, respectively. (*D*) Like *C*, but with 25 μM BAPTA. Note that absolute calcium levels strongly increase as barriers are located increasingly close to the membrane. Most similar calcium levels under both buffer conditions are obtained with the barrier in shell 11. Also note the delayed rise phase kinetics with 25 μM BAPTA compared with the 50 μM EGTA condition.

tions of our experimental data were obtained with a barrier of 1/3000 at 130 nm beneath the membrane (Fig. 10 *B*). Reduced barrier heights yielded a much too strong suppression of release by BAPTA (Fig. 10 *A*). An increased barrier distance made the concentration dependence of release for BAPTA too steep (Fig. 10 *C*). A reduced barrier distance, on the other hand, yielded a very similar dependence of release on buffer concentration for EGTA and BAPTA (Fig. 10 *D*).

These simulations show that the model used here, incorporating a diffusion barrier of 1/1000 to 1/3000 at a distance of 100–200 nm beneath the membrane, adequately describes the kinetics and buffer concentration dependence of release in melanotropes and explains why the large difference in calcium binding rates of EGTA and BAPTA is reflected to only a very limited extent in their effects on release.

DISCUSSION

The present study demonstrates that local saturation of calcium buffers strongly determines the effect of mobile calcium chelators on the release of large dense core vesicles in pituitary melanotropes. Such saturation may to a great extent level the difference between mobile buffers like EGTA and BAPTA. In addition, we demonstrate that not only the amplitude but also the kinetics of calcium-dependent processes are subject to this phenomenon. Buffer saturation will occur due to the existence of diffusion barriers that can be formed, in principle, by any membrane-surrounded organelle. Thus, the influence of mobile calcium buffers on calcium-dependent processes that are not close to the site of calcium entry is determined not only by the properties of the buffer (rate constants, K_D) and diffusion, but to a large extent by submembranous compartmentalization.

The presumption that, in melanotropes, the distribution of calcium ions upon channel opening is determined by local saturation of calcium buffers would strongly differ from the situation in hair cells, where especially high levels of mobile buffers are presumed to shape the calcium transients and limit the spread of micromolar calcium to ~250 nm from the channel mouth (Roberts, 1993, 1994; Hall et al., 1997).

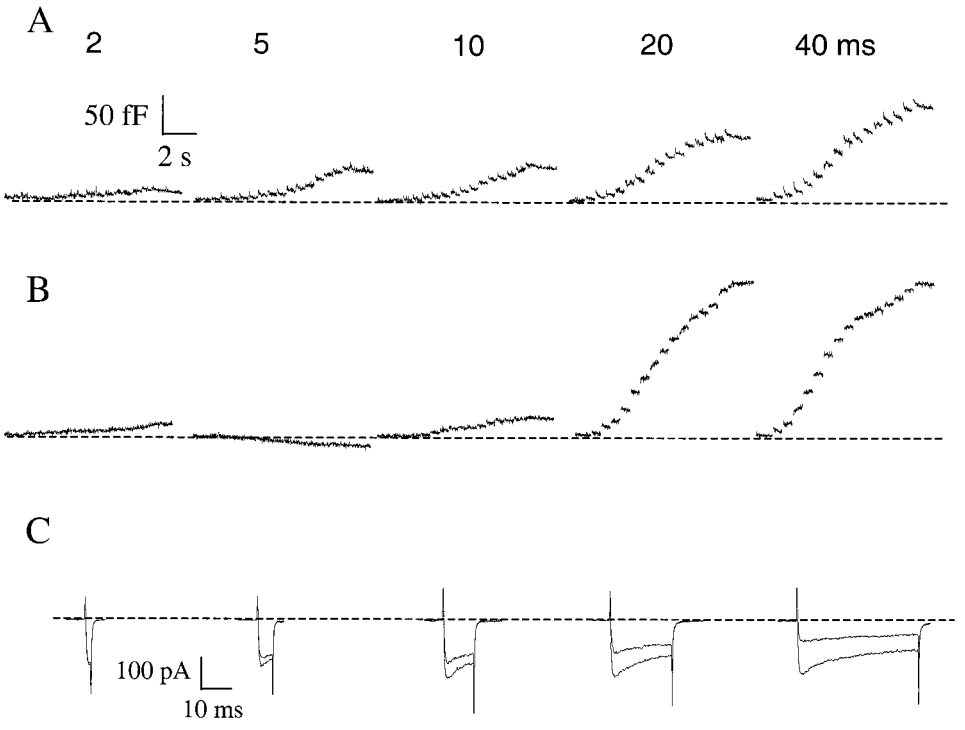

FIGURE 6 Capacitance measurements in rat melanotropes, showing the effect of increasing pulse duration on membrane capacitance. Capacitance recordings were taken during series of 15 repeated depolarizations of durations as indicated (2–40 ms). (*A*) With 50 μM EGTA as calcium buffer. (*B*) Like *A*, but with 25 μM BAPTA as calcium buffer. (*C*) Superimposed calcium current traces induced by the first and last depolarizations of indicated length. Data from the same experiment as in *A*, with 50 μM EGTA. Calcium currents with 25 μM BAPTA are not different.

Results on chromaffin cells (Seward and Nowycky, 1996) and peptidergic nerve terminals (Seward et al., 1995), as well as on neuronal synapses where opening of several calcium channels is required for release of a single vesicle (Borst and Sakmann, 1996), all demonstrated a reduced difference in blocking efficacy of EGTA and BAPTA. This is evidence that the mechanism addressed here might apply more generally. In addition, reduced differences between BAPTA and EGTA in chromaffin cells with respect to the much slower process of threshold secretion (Seward and Nowycky, 1996) are due most likely to their similar affinities, which become relevant on the seconds time scale when calcium levels are in steady-state conditions.

Thus, cells may use or deny mobile buffers in various ways. In some classical, fast synapses, calcium release is determined by microdomains of very rapidly established high levels of calcium (Stanley, 1997; Neher, 1998). Mobile buffers do not affect calcium levels within the microdo-

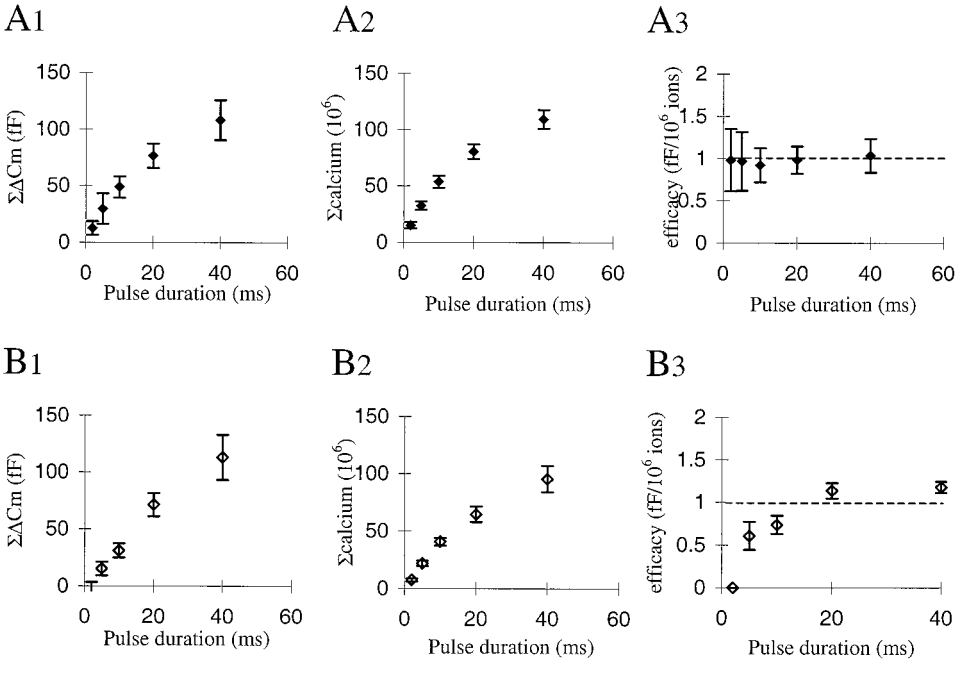

FIGURE 7 Experimentally obtained relationship between pulse duration and efficacy of exocytosis in rat melanotropes. (*A1*) Changes in capacitance as a function of pulse duration. (*A2*) Integral calcium current (number of calcium ions that entered the cell) plotted against pulse duration. (*A3*) Efficacy of calcium ions to stimulate release expressed as changes in capacitance divided by integral calcium current and plotted against pulse duration. Experiments shown in *A1-A3* were performed with 50 μM EGTA as internal calcium buffer. (*B*) Experiments with 25 μM BAPTA.

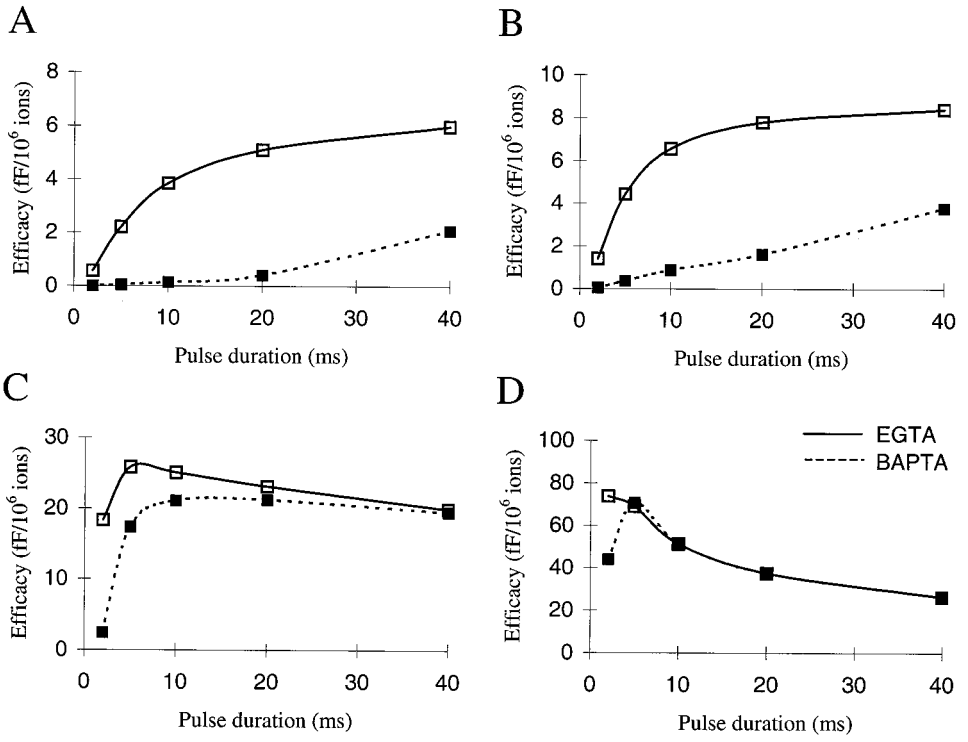

FIGURE 8 Effects of height of the diffusion barriers on the relationship between pulse duration and efficacy of release, expressed as capacitance change per million calcium ions. Barrier is located in shell 11. EGTA = 50 μm, BAPTA = 25 μm. (*A*) Barrier height 1/10. (*B*) Barrier height 1/100. (*C*) Barrier height 1/1000. (*D*) Barrier height 1/10,000. A more or less constant efficacy for EGTA and a rapid increase in efficacy over the first 10 ms is obtained with a barrier of 1/1000 (panel *C*).

mains but cause sharp boundaries of these domains (Hall et al., 1997). Here, the on rate of the buffer determines its influence (Adler et al., 1991). In other synapses and neuroendocrine cells, the average distance between channel and fusion site is larger, possibly because multiple channels are involved in release of a single vesicle. (Borst and Sakmann, 1996; Stanley, 1997; Neher, 1998), resulting in a higher efficacy of buffers but susceptibility to local diffusion barriers. In addition, slow phases of large dense core vesicle release are determined by equilibrium calcium levels that are themselves determined by the affinities of the buffers (Nowycky and Pinter, 1993; Klingauf and Neher, 1997).

Justification for the shell model

In this study, we used a shell model rather than a microdomain model to calculate the spatial and temporal distribution of calcium and calcium buffers. Although the microdomain model (Simon and Llinás, 1985; Llinás et al., 1992; Naraghi and Neher, 1997) accurately describes calcium profiles underneath the membrane around open calcium channels, Klingauf and Neher (1997) showed that the limited extensions of calcium domains of, at most, some tens of nanometers imply that changes in calcium levels at larger distances from the channel are accurately described by a shell model (Sala and Hernandez-Cruz, 1990; Nowycky and Pinter, 1993). In our simulations, a homogenous distribution of calcium channels is assumed with a half-interchannel distance of ~300 nm, for which condition the shell model is valid at >100 nm from the channel. (cf. Fig. 5 *D* in Klingauf and Neher, 1997). Thus, use of a shell model would be justified if the sites of release are located >100 nm from the calcium domains generated by open channels. Experimental data strongly suggest that this is the case for release of large dense core vesicles. In chromaffin cells, secretion of catecholamines upon short depolarizations is slow and prolonged (Chow et al., 1992) and triggered by low micromolar levels of calcium that dissipate only slowly (Chow et al., 1994). Furthermore, in chromaffin cells, calcium chelators slow down exocytosis (Chow et al., 1996). Finally, Klingauf and Neher (1997), in their simulation study, conclude that channels and release sites in chromaffin cells are 200–300 nm apart. Our own data on melanotropes demonstrate that relatively low concentrations of EGTA and BAPTA (800 and 400 μM, respectively) completely block exocytosis (Mansvelder and Kits, 1998; this paper), strongly supporting the argument that calcium ions must travel a substantial distance toward the release site, thus creating a time window in which buffer molecules can act upon them.

This situation contrasts with that in classical, fast synapses, which require low millimolar calcium levels to trigger fusion and have a delay between channel opening and fusion of <200 μs (Llinas et al., 1992; Stanley, 1993). This was taken as evidence that in classical synapses, channels are very closely linked to the release site. The demonstration that N-type channels interact directly with syntaxin (Sheng et al., 1994; Bezprozvanny et al., 1995) as well as synaptotagmin (Leveque et al., 1994) confirmed this hypothesis. As a result, mobile calcium chelators hardly affect synaptic release (Adler et al., 1991; von Gersdorff and Matthews, 1994). These data demonstrate that the coupling between channel and release site differs strongly for fast neuronal

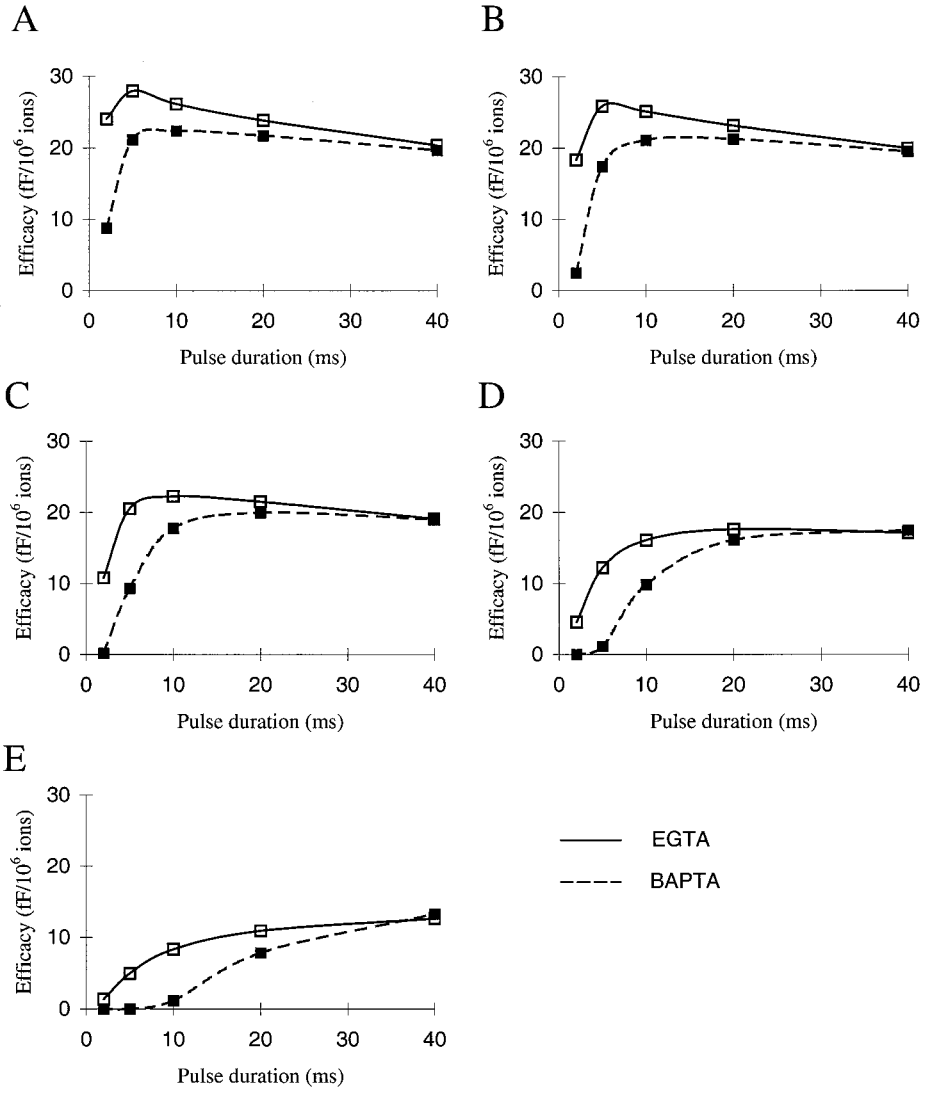

FIGURE 9 Effects of the distance between the diffusion barrier and the membrane on the relationship between pulse duration and efficacy. Barrier height 1/1000; EGTA = 50 μm, BAPTA = 25 μm; (*A*) Barrier location in shell 6. (*B*) Barrier location in shell 11. (*C*) Barrier location in shell 21. (*D*) Barrier location in shell 41. (*E*) Barrier location in shell 81. With a barrier too close to the membrane, the delayed kinetics of changes in $[Ca]_i$ with 25 μM BAPTA are lost. With the barrier too far away from the membrane, the efficacy of release becomes dependent on pulse duration for either buffer.

synapses and neuroendocrine cells, justifying the use of a shell model in the latter but not in the former case.

Limitations of the model

Our simulations rest on a number of assumptions that may limit their validity. First, in the model it is assumed that calcium channels are homogeneously distributed over the cell membrane, giving rise to an equal influx of calcium throughout the cell membrane. However, one cannot exclude the possibility that calcium channels are clustered and that such clusters may lead to calcium domains that are larger in extension and live longer than single-channel domains. Even if channels cluster, though, the data imply that vesicle release takes place at some distance from the channel cluster, so that the mobile buffers can chelate incoming calcium. In this sense, clustering need not induce a fundamental difference. In other words, the assumption of a homogeneous distribution of calcium in each shell in the model does not imply that channels are necessarily distributed homogeneously over the cell membrane. Rather, it implies that the channels are sufficiently far away from the release sites to justify neglect of the inhomogeneities.

Second, we ignored extrusion of calcium through the plasma membrane by calcium pumps. We reasoned that calcium extrusion is relatively slow, and therefore negligible, in the time range of 0–40 ms that we considered. This conforms to the data from Sala and Hernandez-Cruz (1990), who showed that extrusion plays little role in shaping the calcium transient (amplitude, kinetics) in either the outer or inner shells.

Although qualitatively, the model closely predicts experimental results, quantitatively, the model and the experimental data differ with respect to the size of the release response. This discrepancy is most likely explained by possible deviations of numerical values assumed for various parameters from the actual but unknown values in the physiological experiment. Notably, we assumed a readily releasable pool of 250 fF (Thomas et al., 1993a,b; Parsons et al., 1995). This figure, however, is based on experiments

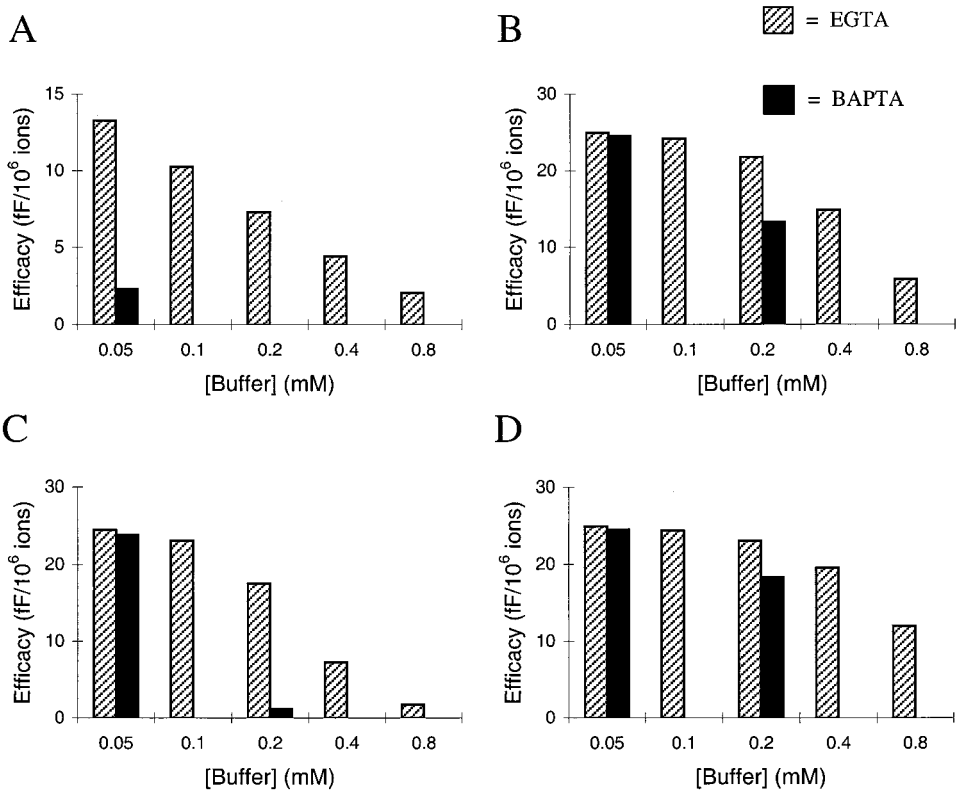

FIGURE 10 Effects of height and location of the diffusion barrier on the relation between buffer concentration and efficacy of exocytosis. Variable EGTA and BAPTA concentrations are indicated. (*A*) Barrier height 1/300, barrier location in shell 11. (*B*) Barrier height 1/3000, barrier location in shell 11. (*C*) Barrier height 1/3000, barrier location in shell 21. (*D*) Barrier height 1/3000, barrier location in shell 6. The best approximation of the experimental results is seen in *B*, where both the relative strength of suppression of release and the dependence on buffer concentration for either buffer match the experimental data.

in which, by means of flash photolysis, a step increase in calcium is imposed throughout the cell. Under experimental conditions the increase in calcium upon a short depolarization may be limited to compartments around the channels, therefore yielding a capacitance increase of only ~10 fF (Mansvelder and Kits, 1998). Thus, the readily releasable pool in these experiments may be limited to the granules docked near calcium channels and therefore smaller than the 250-fF pool (Horrigan and Brookman, 1994). This would imply that our simulations yield larger release responses than the experiments.

Finally, our results pertain to the fast, early phase of exocytosis occurring within 40 ms (and actually allowing detection of release upon a 2-ms pulse). This phase of release is believed to concern only an immediately releasable pool of vesicles that do not require any additional priming apart from the final calcium-dependent steps and the ultimate fusion step. Our model does not take into account depletion or filling of this release-ready pool.

Mobile versus immobile buffers

In general, immobile buffers slow down and prolong the occurrence of calcium-dependent processes because they contribute to initial chelating of ions but release calcium when free levels drop, thus allowing for extended duration of the process. It was shown by Sala and Hernandez-Cruz (1990) that the mobility of the buffers has little influence on the calcium transients in the outermost shells of the cell, but strongly affects those further away from the cell membrane. In particular, increased mobility will result in increased release of calcium by buffer molecules that diffuse from the outer regions toward the inner region of the cell. For microdomains, Naraghi and Neher (1997) showed that fixed buffers do not affect steady state concentrations in calcium microdomains (which is the relevant condition because steady state within a microdomain is obtained within hundreds of microseconds (Roberts, 1994)), but somewhat prolong the time course leading to the steady state condition. Thus, regardless of the model, submembranous calcium transients do not seem to be shaped by fixed buffers. This result corresponds well with conclusions from our simulations showing that unless very high levels of fixed buffers are used, inclusion of fixed buffers does not significantly affect temporal or spatial distribution of calcium. Only very high levels of fixed buffer cause a drop in calcium concentration very close to the membrane. Fixed buffers then become dominant over mobile buffers, which results in equal effects of different concentrations of EGTA and BAPTA close to the membrane. However, these effects bear little relevance to secretion, since the fixed buffer clamps the calcium concentration close to basal levels.

Naraghi and Neher (1997) characterized buffers by means of a buffer length constant (depending on the dissociation constant, concentration, calcium binding rate, and diffusion rate) that describes the average length that a calcium ion will travel before it is captured by the buffer. A faster buffer thus has a shorter length constant. Buffer saturation will be smaller with larger length constants and vice versa. This approach predicts larger saturation for

BAPTA than for EGTA, which in turn will reduce the difference in efficacy of the two buffers. Our simulations show that, in order to cause sufficient saturation to explain the limitations in block of release by EGTA and BAPTA, diffusion barriers may be involved that enhance and prolong calcium transients.

Large dense core vesicle release

The final stage in the release of large dense core vesicles is described by a series of three calcium-dependent steps and an ultimate, calcium-independent fusion step (Neher and Zucker, 1993; Thomas et al., 1993b; Heinemann et al., 1994; Chow et al., 1996). This model concerns exocytosis of predocked or immediately releasable vesicles lying adjacent to the membrane. Both chromaffin cells and melanotropes have been used to investigate this final stage of release. Thomas et al. (1990, 1993a,b) showed, for melanotropes, that upon a step rise in cytosolic calcium to a level of up to 100 μM, exocytosis proceeds in multiple phases, commencing after a 3-ms delay with a fast burst (amplitude 250 fF, time constant 15 ms at 30–34°C). This phase is completed in ~40 ms and corresponds to the fast release of predocked vesicles that we studied here. Neher and Zucker (1993) and Heinemann et al. (1994) performed similar experiments in chromaffin cells with similar results. Parsons et al. (1995) demonstrated that the immediately releasable pool comprises no more than 10% of the total pool of docked vesicles. Both for melanotropes and chromaffin cells, the calcium dependence of fast exocytosis was characterized by a K_D for a single binding site in the low micromolar range (~10 μM), resulting in half-maximal release at levels of ~30–40 μM.

An important observation was that secretion persists for some time after cessation of calcium entry (Chow et al., 1992). Because the secretory process itself is fast (Thomas et al., 1993a,b; Heinemann et al., 1994), Chow et al. (1994, 1996) investigated whether diffusion of calcium ions is responsible for this delay. They demonstrated, for chromaffin cells, that mobile buffers reduce the persistence of secretion and argued that this implies that calcium ions must travel some time to reach the release sites. We obtained similar results for melanotropes (Mansvelder and Kits, 1998). Thus, there is consensus that there is a spatial separation of calcium channels and release sites in neuroendocrine cells, estimated to be 100–200 nm (Roberts, 1994; Klingauf and Neher, 1997; Neher, 1998). Our present results demonstrate that, although this spatial separation allows mobile calcium buffers to affect the release process, the influence of mobile calcium buffers on the amplitude and kinetics of the release response is limited due to the occurrence of (local) saturation of the buffers. Saturation could arise from compartmentalization, which limits free diffusion of calcium and buffer molecules.

In spite of the diffusion distance, calcium channel activation is tightly and efficiently coupled to exocytosis. For short depolarizing pulses (2 ms), this is explained by the slowness of EGTA. (Note that BAPTA blocks release in response to a 2-ms pulse.) For longer pulses, saturation of the buffers prevents block of release, thus allowing a linear relationship between the number of entered calcium ions and release (Mansvelder and Kits, 1998).

The nature of diffusion barriers

The supposition of (local) diffusion barriers is likely to be a valid one regarding the morphological complexity of living cells. Thus, any cell organelle or membranous structure may in fact act as a relative or absolute barrier. Given their size, large dense core granules themselves will act as strong barriers for calcium and buffer molecules. Obviously, the resulting reduced mobility of the buffer molecules is highly relevant, as it occurs at the very spot where release takes place.

However, our hypothesis does not exclude the possibility that other factors are involved in causing buffer saturation. For instance, calcium-induced calcium release may be considered as an alternative or additional process, although there are no reports that it occurs in melanotropes. Moreover, the time scale of the process under consideration (rapid release within a microsecond period) makes it unlikely that calcium-induced calcium release could be of great importance.

HDM was on a grant from the NWO Medical Research Council (903–42-008).

REFERENCES

Adler, E. M., G. J. Augustine, S. N. Duffy, and M. P. Charlton. 1991. Alien intracellular calcium chelators attenuate neurotransmitter release at the squid giant synapse. *J. Neurosci.* 11:1496–1507.

Bezprozvanny, I., R. H. Scheller, and R. W. Tsien. 1995. Functional impact of syntaxin on gating of N-type and Q-type calcium channels. *Nature.* 378:623–626.

Borst, J. G. G., and B. Sakmann. 1996. Calcium influx and transmitter release in a fast CNS synapse. *Nature.* 383:431–434.

Chow, R. H., J. Klingauf, C. Heinemann, R. S. Zucker, and E. Neher. 1996. Mechanisms determining the time course of secretion in neuroendocrine cells. *Neuron.* 16:369–376

Chow, R. H., J. Klingauf, and E. Neher. 1994. Time course of Ca^{2+} concentration triggering exocytosis in neuroendocrine cells. *Proc. Natl. Acad. Sci. USA.* 91:12765–12769.

Chow, R. H., L. von Rüden, and E. Neher. 1992. Delay in vesicle fusion revealed by electrochemical monitoring of single secretory events in adrenal chromaffin cells. *Nature.* 356:60–63.

Fidler Lim, N., M. C. Nowycky, and R. J. Bookman. 1990. Direct measurement of exocytosis and calcium currents in single vertebrate nerve terminals. *Nature.* 344:449–451.

Fidler, N., and J. M. Fernandez. 1989. Phase tracking: an improved phase detection technique for cell membrane capacitance measurements. *Biophys. J.* 56:1153–1162.

Hall, J. D., S. Betarbet, and F. Jaramillo. 1997. Endogenous buffers limit the spread of free calcium in hair cells. *Biophys. J.* 73:1243–1252.

Heinemann, C., R. H. Chow, E. Neher, and R. S. Zucker. 1994. Kinetics of the secretory response in bovine chromaffin cells following flash fotolysis of caged Ca^{2+}. *Biophys. J.* 67:2546–2557.

Hines, M. 1989. A program for simulation of nerve equations with branching geometries. *Int. J. Biomed. Comput.* 34:55–68.

Horrigan, F. T., and R. Brookman. 1994. Releasable pools and the kinetics of exocytosis in adrenal chromaffin cells. *Neuron.* 1119–1129.

Joshi, C., and J. M. Fernandez. 1988. Capacitance measurements: an analysis of the phase detector technique used to study exocytosis and endocytosis. *Biophys. J.* 53:885–892.

Keja, J. A., J. C. Stoof, and K. S. Kits. 1991. Voltage-activated currents through calcium channels in rat pituitary melanotropic cells. *Neuroendocrinology.* 53:349–359.

Keja, J. A., and K. S. Kits. 1994. Single channel properties of high- and low-voltage-activated calcium channels in rat pituitary melanotropic cells. *J. Neurophysiol.* 71:840–855.

Klingauf, J., and E. Neher. 1997. Modelling buffered Ca2+ diffusion near the membrane; implications for secretion in neuroendocrine cells. *Biophys. J.* 72:674–690.

Leveque, C., O. el Far, N. Martin-Moutot, K. Sato, R. Kato, M. Takahashi, and M. J. Seagar. 1994. Purification of the N-type calcium channel associated with syntaxin and synaptotagmin: a complex implicated in synaptic vesicle exocytosis. *J. Biol. Chem.* 269:6306–6312.

Llinas, R., M. Sugimori, and R. B. Silver. 1992. Microdomains of high calcium concentration in a presynaptic terminal. *Science.* 256:677–679.

Mansvelder, H. D., J. C. Stoof, and K. S. Kits. 1996. Dihydropyridine block of ω-Agatoxin IVA and ω-Conotoxin GVIA sensitive Ca^{2+} channels in rat pituitary melanotropic cells. *Eur. J. Pharmacol.* 311:293–304.

Mansvelder, H. D., and K. S. Kits. 1998. The relation of exocytosis and rapid endocytosis to calcium entry evoked by short repetitive depolarizing pulses in rat melanotropic cells. *J. Neurosci.* 18:81–92.

Naraghi, M., and E. Neher. 1997. Linearized buffered Ca^{2+} diffusion in microdomains and its implications for calculation of $[Ca^{2+}]$ at the mouth of a calcium channel. *J. Neurosci.* 17:6961–6973.

Neher, E. 1998. Vesicle pools and Ca2+ microdomains: new tools for understanding their roles in neurotransmitter release. *Neuron.* 20: 389–399.

Neher, E., and R. S. Zucker. 1993. Multiple calcium-dependent processes related to secretion in bovine chromaffin cells. *Neuron.* 10:21–30.

Nowycky, M. C., and M. J. Pinter. 1993. Time courses of calcium and calcium-bound buffers following calcium influx in a model cell. *Biophys. J.* 64:77–91.

Parsons, T. D., J. R. Coorssen, H. Horstmann, and W. Almers. 1995. Docked granules, the exocytotic burst, and the need for ATP hydrolysis in endocrine cells. *Neuron.* 15:1085–1096.

Roberts, W. M. 1993. Spatial calcium buffering in saccular hair cells. *Nature.* 363:74–76.

Roberts, W. M. 1994. Localization of calcium signals by a mobile calcium buffer in frog saccular hair cells. *J. Neurosci.* 14:3246–3262.

Sala, F., and A. Hernandez-Cruz. 1990. Calcium diffusion modelling in a spherical neuron: relevance of buffering properties. *Biophys. J.* 57: 313–324.

Schweizer, F. E., H. Betz, and G. J. Augustine. 1995. From vesicle docking to endocytosis: intermediate reactions of exocytosis. *Neuron.* 14: 689–696.

Seward, E. P., N. I. Chernevskaya, and M. C. Nowycky. 1995. Exocytosis in peptidergic nerve terminals exhibits two calcium sensitive phases during pulsatile calcium entry. *J. Neurosci.* 15:3390–3399.

Seward, E. P., and M. C. Nowycky. 1996. Kinetics of stimulus-coupled secretion in dialyzed bovine chromaffin cells in response to trains of depolarizing pulses. *J. Neurosci.* 16:553–562.

Sheng, Z. H., J. Rettig, M. Takahashi, and W. A. Catterall. 1994. Identification of a syntaxin-binding site on N-type calcium channels. *Neuron.* 13:1303–1313.

Simon, S. M., and R. Llinás. 1985. Compartimentalization of the submembrane calcium activity during calcium influx and its significance in transmitter release. *Biophys. J.* 48:485–498.

Smith, P. D., G. W. Liesegang, R. L. Berger, G. Czerlinski, and J. Podolsky. 1984. A stopped-flow investigation of calcium ion binding by ethylene glycol bis(b-aminoethyl ether)-N,N,-tetraacetic acid. *Anal. Biochem.* 143:188–195.

Stanley, E. F. 1993. Single calcium channels and acetylcholine release at a presynaptic nerve terminal. *Neuron*. 11:1007–1011.

Stanley, E. F. 1997. The calcium channel and the organization of the presynaptic transmitter release face. *Trends Neurosci.* 20:404–409.

Thomas, P., A. Suprenant, and W. Almers. 1990. Cytosolic Ca2+, exocytosis, and endocytosis in single melanotrophs of the rat pituitary. *Neuron.* 5:723–733.

Thomas, P., J. G. Wong, and W. Almers. 1993a. Millisecond studies of secretion in single rat pituitary cells stimulated by flash photolysis of caged Ca^{2+}. *EMBO J.* 12:303–306.

Thomas, P., J. G. Wong, A. K. Lee, and W. Almers. 1993b. A low affinity Ca^{2+} receptor controls the final steps in peptide secretion from pituitary melanotrophs. *Neuron.* 11:93–104.

Tsien, R. Y. 1980. New calcium indicators and buffers with high selectivity against magnesium and protons: design, synthesis, and properties of prototype structures. *Biochemistry.* 19:2396–2404.

von Gersdorff, H., and G. Matthews. 1994. Dynamics of synaptic vesicle fusion and membrane retrieval in synaptic terminals. *Nature*. 367: 735–739.

Zucker, R. S. 1996. Exocytosis: a molecular and physiological perspective. *Neuron.* 17:1049–1055.